

# RAINFALL ALGORITHM INVARIANT TO THE WEATHER RADAR OPERATING FREQUENCY AND IMMUNE TO VARIABILITY IN RAINDROP SHAPE-SIZE MODEL

E. Gorgucci and L. Baldini

Istituto di Scienze dell'Atmosfera e del Clima  
Via Fosso del Cavaliere, 100 – 00133 Roma, Italy

## 1. INTRODUCTION

Polarization diversity radar measurements such as reflectivity factor, differential reflectivity, and differential propagation phase are extensively used in rainfall estimation (Bringi and Chandrasekar 2001). Algorithms to estimate rainfall from polarimetric radar measurements are based on the assumption of a model describing the raindrop shape as a function of drop diameter. Deviation of the prevailing raindrop shape from the assumed model has a direct impact on the accuracy of radar rainfall estimates. Moreover, rainfall algorithms can be only used at the specific radar band frequency for which they have been developed.

A rainfall algorithm for estimating rainfall rate from polarimetric radar data without an a priori assumption about the specific form of mean raindrop shape-size model is presented. This algorithm, obtained from  $Z_h$  and  $Z_{dr}$ , is invariant in the frequency domain ranging from S- to X-band.

Reconstructed profiles obtained from real radar observations are used to validate the rainfall algorithm. For a comparative analysis, two other algorithms based on  $Z_h$  and  $Z_{dr}$  have been found assuming fixed drop shape-size relations and r frequency. The comparison shows that, in the presence of raindrops described by the model of Pruppacher and Beard (1970) or Beard and Chuang (1987), the new rain algorithm follows the DSD variability better than the rain algorithm obtained from a fixed non-linear shape-size model.

## 2. RADAR POLARIMETRIC MEASUREMENTS AND THEIR RELATION TO RAIN MICROPHYSICS

Dual-polarization radar measurements  $Z_h$ ,  $Z_{dr}$  and  $K_{dp}$  are influenced by drop size distribution (DSD) and drop shape. The normalized form of the gamma DSD was introduced to compare the probability density function of  $D$  in the presence of varying water contents (Willis 1984; Illingworth and Blackman 2002). The corresponding form of the gamma DSD can be expressed as

$$N(D) = N_w f(\mu) \left( \frac{D}{D_0} \right)^\mu \exp \left[ - (3.67 + \mu) \frac{D}{D_0} \right] \quad (1)$$

where  $f(\mu)$  is a dimensionless function of  $\mu$ . One interpretation of  $N_w$  is that it is the intercept of an equivalent exponential distribution with the same water content.  $D_0$  is the median volume diameter and  $\mu$  is the shape factor.

For weather radar applications the shape of raindrops can be approximated by oblate spheroids described by the semimajor axis  $a$  and semiminor axis  $b$ . Several equations relating the axis ratio  $r = b/a$  with drop diameter have been proposed. Gorgucci et al. (2000) proposed an approximation of the form

$$r(D) = 1.03 - \beta D \quad (2)$$

with  $r=1$  for  $D \leq 0.03/\beta$ . The linear fit to the wind tunnel data of Pruppacher and Beard (1970) corresponds to  $\beta=0.062 \text{ mm}^{-1}$  (the drop-shape model corresponding to this

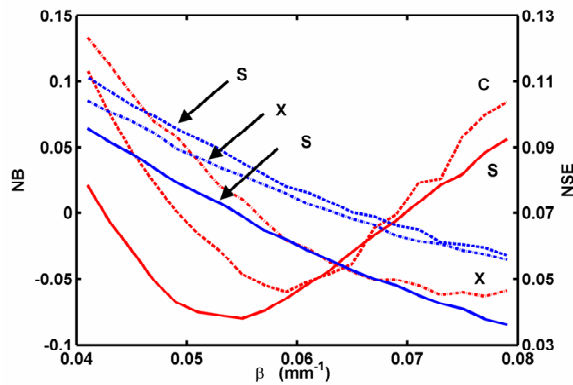


**Figure 1:** Error analysis of the performance of the algorithm (22) as a function of  $\beta$  and for the three wavelengths corresponding to S- (solid line), C- (dashed line), and X- band (dashed-dot line) due to the DSD variability. The analysis was obtained by dividing  $\beta$  into classes and computing in each class the average values of NSE (red lines) and NB (blue lines).

value of  $\beta$  will be henceforth referred to as PB). If the mean axis ratio versus  $D$  relation is nonlinear, it is always possible to define a linear relation that results in the same  $K_{dp}$  (Bringi et al. 2003).

Investigating the relation among radar polarimetric measurements and rain microphysics, Gorgucci et al. (2006), following Bringi and Chandrasekar (2001) and Jameson (1985), expressed the ratio  $K_{dp}/Z_h$  as a function of the parameters  $D_0$  and  $\mu$  of (1) and the mass-weighted mean axis ratio. Using properties of the gamma function, and assuming (2) this relation can be modified in terms of the drop-shape slope factor  $\beta$  and the reflectivity-weighted mean drop diameter  $D_Z = E\{D D^6\} / E\{D^6\}$  as

$$\frac{K_{dp}}{Z_h} = C \frac{\Gamma(4 + \mu)}{\Gamma(7 + \mu)} (7 + \mu)^2 (4 + \mu) \frac{\beta}{\lambda D_Z^2} \quad (3)$$

An empirical relationship between  $Z_{dr}$  and the reflectivity-weighted axis ratio defined as  $r_Z = E\{r D^6\} / E\{D^6\}$  was proposed by Jameson (1983). An approximate form of that relation can be attained as

$$\xi_{dr} = 1 + p(\beta D_Z)^q \quad (4)$$

where  $Z_{dr} = \log_{10}(\xi_{dr})$ . Parameters  $p$  and  $q$  can be found using the simulation described in the next section and result equal to 0.687 and 1.184, respectively. Replacing (4) in (3) and using the moment properties of the normalized gamma DSD, it is possible to derive the relation

$$\beta = \left[ \frac{1}{C' \cdot g(\mu)} \frac{\lambda K_{dp}}{Z_h} \right]^{1/3} (\xi_{dr} - 1)^{2/(3q)} \quad (5)$$

where  $C'$  is a constant and  $g(\mu)$  is a slowly increasing function of  $\mu$  that can be approximated by its average value 0.92. Eq. (5) states that in a domain defined by the three radar variables  $Z_h$ ,  $Z_{dr}$ , and  $K_{dp}$ , these are constrained to take up a limited region of the domain unequivocally defined by the same slope factor.

### 3. PRACTICAL ISSUES FOR $\beta$ ESTIMATION

Equation (5) is valid from S- to X-band if resonance effects are not taken into account. In order to consider such effects, for the three more common weather radar frequencies of 3 GHz (S-band), 5.4 GHz (C-band), and 9.3 GHz (X-band), a simulation was built on the following conditions: *i*) the shape size relation is described by (2) with  $\beta$  ranging between 0.04 and 0.08 mm<sup>-1</sup>; *ii*) gamma DSD parameters vary in the range defined by  $0.5 < D_0 < 3.5$  mm;  $3 < \log_{10} N_w < 5$ ;  $-1 < \mu < 5$ ; *iv*) radar measurements are constrained to  $(10 \log_{10} Z_h) < 55$  dBZ and  $R < 300$  mm h<sup>-1</sup>; *v*) drops are assumed to be oriented with the mean and standard deviation equal to zero 10°, respectively (Bringi and Chandrasekar 2001). Equation (5) presents some practical problems. In fact, when  $K_{dp}$  tends to zero, due to the signal fluctuation, its values can be negative. Moreover, when  $Z_{dr}$  approaches zero, the quantity  $(\xi_{dr} - 1)$  can assume negative values and then (5) becomes meaningless. Therefore,  $(\xi_{dr} - 1)$  was replaced by  $(\xi_{dr} - \kappa)$  and the resulting equation is studied as a function of  $\kappa$ . It can

be seen that  $\kappa$  does not have a big influence on merit factors since the maximum variation of the NSE is 2%. For this reason, in the following,  $\kappa = 0$  is assumed and the following equation will be considered

$$\beta = a \left( \lambda \frac{K_{dp}}{Z_h} \right)^b \xi_{dr}^c \quad (6)$$

Figure 1 shows an error analysis of the performance of the algorithm (5) as a function of  $\beta$  due to the DSD variability and for three wavelengths corresponding to S- (solid line), C- (dashed line), and X-band (dash-dot line). The analysis is obtained by dividing  $\beta$  into classes and computing in each class the average values of NSE (black lines) and NB (light grey lines). The NSE accuracy as a function of  $\beta$  shows different profiles varying with the radar operating frequency. In fact, at S-band the minimum value of the NSE in correspondence with  $\beta = 0.055 \text{ mm}^{-1}$  moves toward higher values of  $\beta$  as the frequency increase to C- and X-band. Figure shows that, for all frequencies, NSE can be estimated with an accuracy ranging between 4% and 7% when  $\beta$  moves between  $0.055 \text{ mm}^{-1}$  and  $0.07 \text{ mm}^{-1}$ . Over the same  $\beta$  interval, the NB presents an overestimation of about 4% at C- and X-band and an underestimation of 6% at S-band.

#### 4. IMPLICATIONS FOR RAIN ESTIMATION

Rainfall algorithms consistent with equation (6) can be built for the operating frequency domain of weather radars. A simple algorithm using  $Z_h$ , and  $Z_{dr}$  optimized for the three weather radar frequencies may be of the form

$$R_Z = a_Z \beta^{b_Z} Z_h^{c_Z} \xi_{dr}^{d_Z}. \quad (7)$$

The parameters of (7) can be found by a nonlinear regression analysis using the simulation described in the previous section. The coefficients  $a_Z$ ,  $b_Z$ ,  $c_Z$ , and  $d_Z$  are 12.63,

2.57, 0.936, and -4.218, respectively. The NSE of (7) is 20% and the correlation coefficient is 99%.

An algorithm using  $K_{dp}$  optimized for the three bands can be expressed using  $(\lambda K_{dp})$  as:

$$R_K = a_K \beta^{b_K} (\lambda K_{dp})^{c_K}. \quad (8)$$

Coefficients  $a_K$ ,  $b_K$ , and  $c_K$  resulting from the simulation described before are 12.63, 1.21, and 0.96, respectively. Eq. (8) presents an NSE of 31.9 % and a correlation coefficient of 97%. From a general point of view, (6), (7), and (8) establish a transform coordinate system that relates the radar parameters  $Z_h$ ,  $Z_{dr}$ ,  $\beta$  or  $K_{dp}$ ,  $\beta$ , and  $\lambda$  to rain rate under the control of a generalized self-consistency relation defined in the domain  $Z_h$ ,  $Z_{dr}$ ,  $\beta$ ,  $K_{dp}$ , and  $\lambda$ .

Due to the lower NSE and to the higher correlation coefficient, (7) shows better ability than (8) to take into account the DSD variations. For this reason, this study focuses only on (7), henceforth indicated as  $\beta$  algorithm. Eq. (7) is compared with standard algorithms obtained assuming nonlinear raindrop shape-size relations. Among the relations available in the literature, those recently proposed by Brandes et al. (2002) and Thurai et al. (2007) (henceforth BZV and THBRS, respectively) are considered in the analysis. Coefficients of standard rain algorithm

$R = a_1 \beta^{b_1} Z_h^{c_1}$  were obtained using the same simulation described in Sect 3, except that shape of raindrops follows the BZV and THBRS model. For the latter, accordingly to Thurai et al. (2007), for  $0.7 \leq D \leq 1.5 \text{ mm}$  has been used the relation of Beard and Kubesh (1991), whereas below 0.7 mm drops have been assumed to be spherical. Specific coefficients for S-, C- and X-bands were derived. Both parameterizations are characterized by very high correlation coefficients, negligible bias, and low NSEs. For both BZV and THBRS, NSE is 13%, 17% at C- and X band. At C-band, NSE of

**Table 1:** NB and NSE of rainfall estimations obtained using the BZV, THBRS, and  $\beta$  algorithms with respect to the corresponding true value for raindrops following the PB or BC shape-size model and for  $Z_h$ ,  $Z_{dr}$ , and  $K_{dp}$  measurements at S- or C- or X-band (with measurement errors)

Profiles		Rain Algorithms					
<b>Drop-shape</b>	Band	BZV		THBRS		$\beta$	
		NB	NSE	NB	NSE	NB	NSE
<b>PB</b>	S	-0.210	0.363	-0.181	0.339	0.111	0.342
	C	-0.158	0.354	-0.134	0.339	0.140	0.332
	X	-0.305	0.438	-0.278	0.411	0.090	0.298
<b>BC</b>	S	-0.085	0.266	-0.046	0.255	-0.025	0.270
	C	-0.064	0.268	-0.036	0.262	-0.023	0.249
	X	-0.152	0.332	-0.116	0.318	-0.057	0.284

BZV is 16% and that of THBRS is 14%. Correlation coefficient is always above 99%. In comparison with the  $\beta$  algorithm, while the correlation coefficients are similar, the NSEs of this algorithm are greater than that of THBRS of about 7%, 3% and 6 % at S-, C- and X-band, respectively. For BZV, increases are 7%, 3%, and 4%.

It must be pointed out that the coefficients of the BZV and THBRS algorithms are specific for each considered frequency, while the the  $\beta$  algorithm have a unique set of coefficients for all three frequency bands. This is because the  $\beta$  shape factor works as a normalizing factor for  $Z_{dr}$  with respect to the drop shape, making it independent from the operating radar frequency.

## 5. VALIDATION

The impossibility of testing the proposed algorithm with respect to all the implications rising from the electromagnetic and microphysical aspects of the problem by directly using real radar polarimetric measurements, forces this study to adopt a simulation. Radar profiles are generated from real profiles collected by the NCAR S-POL radar during the TEFLUN-B campaign following Chandrasekar et al. (2006). The

considered rain profiles correspond to a 15 km-long path containing 100 range bins spaced 0.150 m apart over which the differential phase increase is greater than 6 degrees. Gorgucci et al. (2006) observing the mean shape of raindrops resulting from radar measurements in Florida and in Italy, observed that oblateness of raindrops varies between the PB and the BC model. Therefore, for each of the three weather radar bands, two distinct sets of profiles were constructed assuming these two models. To take into account the different error structures of the different radar measurements, random signal fluctuation is generated in such a way that the measurement errors of  $Z_h$ ,  $Z_{dr}$ , and  $\Phi_{dp}$  correspond to 1 dB, 0.2 dB, and 4 degrees, respectively. The differential phase on backscattering is added to the differential phase profiles.

Fixed a weather radar frequency, for each profile, the path-averaged values  $Z_h$ ,  $Z_{dr}$  and  $K_{dp}$  are computed with and without measurement errors, and used to obtain the mean values of  $\beta$  from (6). Then, this  $\beta$  is used to compute the rain rate in each range bin with (7) and with the corresponding relations derived from the BZV and THBRS algorithm for each band.

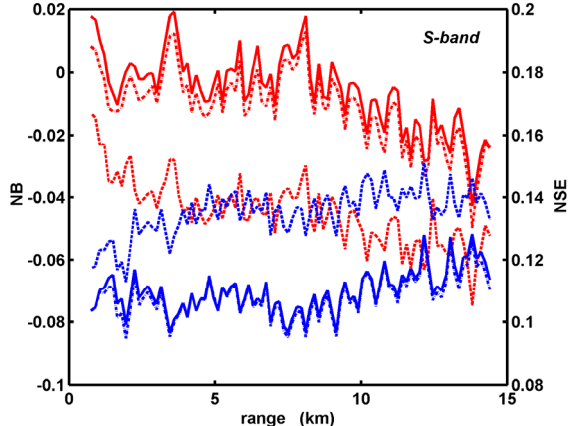


**Figure 2:** NSE (red lines) and NB (blue lines) of rainfall estimate obtained using BZV (dash-dot line), THBRS (dashed line), and  $\beta$  algorithm (solid line) due only to the DSD variability. Rain profiles are obtained at S-band with raindrops following the BC model. Measurement errors are not included

Figure 2 shows the NSE and NB of rain computed with respect to the true rainfall rate as a function of range for BZV, THBRS, and  $\beta$  algorithms, for the case that raindrops follow the BC model and for S-band. Measurement errors are not included in order to compare algorithms with respect to DSD variations only. Given that BC and THBRS shape-size models are quite similar, the THBRS algorithm presents the best performance along the range, with an average NSE of about 14%, pointing out a better ability to describe the variability of the raindrops than BZV and  $\beta$  algorithms, characterized by an average NSE of 17%. Results for PB rain profiles (not shown) indicate again that the  $\beta$  algorithm meets the DSD variability requirements better than the BZV and THBRS algorithms.

Results obtained with measurement errors are summarized in Table 1 that compares the different algorithms in terms of NB and NSE of rainfall estimation for range profiles simulated assuming raindrops following the PB or BC shape-size models, for S- or C- or X-band. It is worth remarking that attenuation effects on  $Z_h$  and  $Z_{dr}$  measurements at C- and X- band are not considered in this study. When raindrops follow the PB model, the NSE of the  $\beta$

algorithm presents values that are comparable to the THBRS algorithm at S- and C-band and is lower than 10% at X-band. Regarding the NSE of the BZV algorithm, they present values of about 2% more than THBRS. With regard to NB of the  $\beta$  algorithm, it demonstrates better results when compared to the BZV and THBRS algorithms. This performance is because the  $\beta$  algorithm, using the self-consistency principle, produces a kind of tuning for the radar measurements that minimizes the biases. In fact, even though the THBRS algorithm presents values lower than the BZV algorithm, they are 7% and 18% greater than those obtained with the  $\beta$  algorithm for S- and X-band, and are comparable at C-band. Once again, it must be recalled that the lower NB differences at C-band between the different algorithms may be determined by the effects of resonance scattering that may reduce any consistency among  $Z_h$ ,  $Z_{dr}$ , and  $K_{dp}$ .

In the presence of raindrop media following the BC model and measurement errors, the NSE of the BZV and THBRS algorithm, due to the closeness of BZV and THBRS to the BC equilibrium shape, is a little better than that of the PB model. In fact, the NSEs of the BZV and THBRS algorithms are lower at 0.4% and 1.5% than the  $\beta$  algorithm at S-band, whereas they are greater than 1.9% and 1.3% at C-band. For the X-band, the NSE of the  $\beta$  algorithm is lower at 3.4% and 4.8% than the THBRS and BZV algorithm, respectively. With regard to the NB, once again, the  $\beta$  algorithm shows the best performance, with values lower than 2% and 6% at S-band, 1.3% and 4% at C-band, 5.9% and 10.5% at X-band for the THBRS and BZV algorithms, respectively.

A general result of the analysis is that, in the presence of the raindrops whose shape is described by the PB or BC models, the  $\beta$  algorithm follows the DSD variability much better than the THBRS and BZV algorithms. Due to the different weight of the

measurement errors on the three algorithms, the  $\beta$  algorithm presents a reduction in the ability to take into account the DSD variability even though its performance remains comparable to or better than the other two. Finally, an important result is that the  $\beta$  algorithm presents the lowest NB, both for PB and BC models, at S-, C- and X-band.

## REFERENCES

- Beard K. V., and C. Chuang, 1987: A new model for the equilibrium shape of raindrops. *J. Atmos. Sci.*, 44, 1509–1524.
- Brandes, E. A., G. Zhang, and J. Vivekanandan, 2002: Experiments in rainfall estimation with a polarimetric radar in a subtropical environment. *J. Appl. Meteor.*, 41, 674–685.
- Bringi, V. N. and V. Chandrasekar, 2001: Polarimetric Doppler weather radar: Principles and applications. Cambridge University Press, 648 pp.
- Bringi, V. N., V. Chandrasekar, J. Hubbert, E. Gorgucci, W. L. Randeu, and M. Schoenhuber, 2003: Raindrop size distribution in different climatic regimes from disdrometer and dual-polarized radar analysis. *J. Atmos. Sci.*, 60, 354–365.
- Chandrasekar, V., S. Lim, and E. Gorgucci, 2006: Simulation of X-band rainfall observations from S-band radar data, *J. Atmos. Oceanic Technol.*, 23, 1195–1205.
- Gorgucci, E., G. Scarchilli, V. Chandrasekar and V. N. Bringi, 2000: Measurement of mean raindrop shape from polarimetric radar observations. *J. Atmos. Sci.*, 57, 3406–3413.
- Gorgucci, E., L. Baldini, and, V. Chandrasekar, 2006: What is the shape of raindrops? An answer from radar measurements. *J. Atmos. Sci.*, 63, 3033–3044.
- Jameson, A. R., 1983: Microphysical interpretation of multi-parameter radar measurements in rain. Part I: Interpretation of polarization measurements and estimation of raindrop shapes. *J. Atmos. Sci.*, 40, 1792–1802.
- Jameson, A. R., 1985: Microphysical interpretation of multi-parameter radar measurements in rain. Part III: Interpretation and measurement of propagation differential phase shift between orthogonal linear polarizations. *J. Atmos. Sci.*, 42, 607–614.
- Beard K. V., and R. J. Kubesh, 1991: Laboratory measurements of small raindrop distortion. Part II: Oscillation frequencies and modes. *J. Atmos. Sci.*, 48, 2245–2264.
- Pruppacher, H. R. and K.V. Beard, 1970: A wind tunnel investigation of the internal circulation and shape of water drops falling at terminal velocity in air. *Quart. J. Roy. Meteor. Soc.*, 96, 247–256.
- Scarchilli G., E. Gorgucci, V. Chandrasekar, and A. Dobaie, 1996: Self-consistency of polarization diversity measurement of rainfall. *IEEE Trans. Geosci. Remote Sens.*, 34, 22–26.
- Thurai, M., G. J. Huang, V. N. Bringi, W. L. Randeu and M. Schönhuber, 2007: Drop shapes, model comparisons, and calculations of polarimetric radar parameters in rain. *J. Atmos. Oceanic Technol.*, 24, 1019–1032.
- Willis, P. T., 1984: Functional fits to some observed drop size distributions and parameterization of rain. *J. Atmos. Sci.*, 41, 1648–1661.

## Acknowledgements

This research was supported by the Italian Ministry of University and Research through the AEROCLOUDS project and by the Civil Protection Department of the Presidency of the Council of Ministers of Italy.